Soft Matter

Cite this: *Soft Matter*, 2012, **8**, 2907

www.rsc.org/softmatter

PAPER

Spectroscopic study of the microstructure and phase transition of regioregular poly(3-dodecylthiophene)†

Yan Guo, Yin Jin and Zhaohui Su*

Received 16th November 2011, Accepted 4th January 2012
DOI: 10.1039/c2sm07191f

Regioregular poly(3-dodecylthiophene) (P3DDT) films were studied by temperature-dependent FTIR and DSC. Structural evidence was presented to confirm that the endothermic transition observed by DSC at ~60 °C is side chain melting. New vibrational bands of the C_β-H out-of-plane bending were identified and correlated to various structures of P3DDT: the component at 827 cm^{-1} was assigned to the form II modification; the 806-cm^{-1} band was ascribed to an intermediate phase with twisted main chains and ordered side chains, and the component at 800 cm^{-1} was due to doped segments. Based on temperature-dependent spectroscopic analysis, a detailed description of the microstructure and phase transition of P3DDT is presented.

Introduction

In recent years, polythiophenes have become one of the most attractive conjugated polymers with potential application in the areas of electronics and optoelectronics due to its stability and versatility.[1–3] Solubility and fusibility of polythiophene are dramatically improved by modifying the rigid thienyl backbone of the polymer with flexible alkyl side chains, which also leads to rich morphologies and properties.[3–5] Poly(3-alkylthiophene)s (P3ATs), especially the regioregular ones, have been widely used in organic solar cells and field-effect transistors due to their processability and high charge-carrier mobility,[4–7] and the performance of P3ATs in these devices is controlled by microstructures formed during processing.[6,8]

Thermal treatment has been introduced to modulate the microstructure of P3AT films and significantly improve the performance of the devices,[4,9] therefore, microstructure and temperature-dependent structure evolution of P3ATs have been the focus of extensive research for a long time.[10–12] However, the ordered and disordered structures of the rigid backbone and the flexible side chains still are not well understood, especially the structure and transition concerning the alkyl side chains. Phase transitions of P3ATs have been studied by differential scanning calorimetry (DSC), which reveals that the thermal behavior of P3ATs depends on the length of the side chain[13,14] and molecular weight of the polymer.[15,16] In particular, for P3ATs with long alkyl side chains, such as poly(3-dodecylthiophene) (P3DDT), there exists two distinct phase transitions as observed by DSC; the transition at higher temperature is unambiguously assigned to the melting/crystallization of the main chain, and the one at lower temperature is presumed to be that of the side chains.[14,17–19] Pankaj *et al.* investigated P3ATs with different regioregularities and side chain lengths of 6–12 carbons, and observed the low temperature transition, attributed to weak side chain crystallization, only in P3DDT.[19,20] On the other hand, Wu *et al.* studied poly(3-hexylthiophene) (P3HT) by DSC and X-ray diffraction (XRD), and observed for a sample with a relatively low molecular weight of ~3 K a phase transition at ~60 °C by DSC; based on the disappearance of several (hk0) diffractions in the XRD pattern above this temperature, they assigned the transition to the melting of hexyl side chains, while such a transition was absent in P3HTs with higher molecular weights.[16] Recently in a preliminary report, we presented first spectroscopic evidence of side-chain melting/crystallization in P3DDT and absence of such in P3HT.[21]

Like other semicrystalline polymers, there are amorphous and ordered domains in P3AT films.[16] Because of the rigidity of the backbone and immiscibility between the main chains and the side chains, P3ATs tend to form lamellar structures with π-stacked main chains alternating with alkyl side chains. Two different crystal modifications, form I and form II, have been reported.[22] Form I is the more common crystalline polymorph, obtained under typical film preparation conditions such as casting or spin-coating from chlorinated solutions. Form II is more likely found in P3ATs with long alkyl side chains, low molecular weights and low regioregularities,[23,24] which exhibits a (100) Bragg diffraction peak in the XRD pattern at a higher angle than form I attributed to reduced interlayer distance in the direction of side chains. For example, form II of poly(3-octylthiophene) (P3OT) and P3DDT

State Key Laboratory of Polymer Physics and Chemistry, Changchun Institute of Applied Chemistry, Chinese Academy of Sciences, 5625 Renmin Street, Changchun, 130022, People's Republic of China. E-mail: zhsu@ciac.jl.cn; Fax: + 86-431-85262126; Tel: +86-431-85262854

† Electronic Supplementary Information (ESI) available: IR spectral reproducibility, and additional peak shift and intensity variation data. See DOI: 10.1039/c2sm07191f/

are obtained in films fabricated by slow evaporation of solvent, which upon heating transforms to form I at a temperature lower than the melting point, and does not reappear on cooling.[23] Form II has also been discovered in poly(3-butylthiophene) (P3BT) and P3HT films annealed in solvent vapor.[25,26] Recently, another crystal modification, form I′, was proposed for P3BT,[27] which was found in both P3BT and P3HT films prepared by slow solvent evaporation at low temperatures.[28,29]

Vibrational spectroscopy is capable of providing rich information on local structures in polymeric systems, and has been applied extensively to understand structure and thermal behavior of P3ATs at molecular level. For instance, Zerbi *et al.* observed by FTIR and Raman that two phases exist in P3HT and P3OT samples at room temperature, and upon heating the disordered phase increases with both the side chains and the main chains becoming twisted.[11,30] Tashiro *et al.* investigated P3HT and P3DDT by temperature-dependent FTIR in conjunction with XRD and UV-vis, and supposed that the *gauche* conformation of the side chains increases with temperature, which induces disorder of the main chain and decrease of the conjugation length.[31] In a series of works, Asakawa and co-workers focused on peak shifts of the C_β-H out-of-plane bending band to investigate the dynamics of the twist motion of the main chain of P3BT and P3HT, and proposed a phase diagram of P3ATs.[32–34] Recently, by using FTIR with XRD and DSC, Yuan *et al.* investigated P3BT and P3HT films prepared at slow solvent evaporation rates. They reported a new component of the C_β-H out-of-plane bending vibration and assigned it to form I′ polymorph, and observed the form I′-to-form I phase transition for both polymers.[28,29] Despite these excellent works, confusions exist concerning assignments of some important vibrational bands, especially the overlapping C_β-H out-of-plane bending band which associates with multiple phases of P3ATs, and spectroscopic characteristics for form II modification are not yet available for further structure studies.

In this paper, structures associated with the alkyl side chains and the main chain in P3DDT as well as their evolution with temperature are investigated by temperature-dependent FTIR spectroscopy in conjunction with DSC and XRD. FTIR is particular useful here because it can track in real time structure changes of the thienyl backbone and the alkyl side chains separately, as well as the transformation between various phases including the amorphous phase. Spectroscopic evidence for side-chain melting is discussed, and several new vibrational bands are identified and correlated to various structures, with the aid of which temperature-dependent microstructure of P3DDT is determined.

Experimental section

Regioregular P3DDT (Mw = 59 000, PDI = 1.6, 93% H–T) was purchased from Rieke Metals Inc. and used without further purification. Molecular weight was determined by GPC with THF as the solvent against polystyrene standards. H–T regioregularity was measured by nuclear magnetic resonance (NMR) spectroscopy *via* the ratio of the signals at 2.8 and 2.6 ppm.[7]

A chloroform solution of P3DDT (10 mg mL^{-1}) was cast onto substrates and allowed to dry for several minutes at ambience to yield thin films. FTIR measurements were carried out on a Nicolet 6700 spectrometer equipped with a MCT detector. A Linkam FTIR-600 hot stage was employed to control the temperature with an accuracy of ±0.1 °C. A P3DDT film on KBr disc was mounted in the heating cell and heated from 20 to 180 °C, held for 5 min, and then cooled to 20 °C, with a heating/cooling rate of 3 °C min^{-1}. A spectrum was acquired every 5 °C by averaging 16 scans at a resolution of 4 cm^{-1}. The data were analyzed using OPUS software, and curve-fitting was performed using the Levenberg–Maguardt algorithm based on the least squares method. The 2D Pocha program written by Daisuke Adachi (Kwansei Gakuin University) was used for two-dimensional (2D) correlation analysis. In contour plots, the averaged one-dimensional reference spectrum is depicted at the left and top; the 2D correlation spectrum is in the center, and positive and negative correlation intensities are denoted by the unshaded area (red) and shaded area (black).

P3DDT films cast on glass substrates were scraped off for thermal analysis. DSC measurements were conducted on a TA Q100 calorimeter in nitrogen atmosphere. The temperature program was identical to that for FTIR experiments. XRD patterns were recorded on a Bruker D8 Discover with a copper target ($\lambda_{k\alpha}$ = 0.154 nm) at 2θ of 2∼30° at a scan rate of 1°/min.

Results and discussion

The chemical structure of regioregular P3DDT is depicted in Scheme 1. A typical FTIR spectrum of P3DDT film cast from solution and dried at ambience is displayed in Fig. 1a. Obviously, the spectrum mainly includes three regions: 3100–2800 cm^{-1}, C–H stretching (ν(C–H)); 1530–1300 cm^{-1}, C=C stretching, and CH_2 and CH_3 bending and wagging; 900–700 cm^{-1}, methyl rocking, C_β-H out-of-plane bending (δ(C_β-H)), and $(CH_2)_n$ in-phase rocking (γ$(CH_2)_n$).[35,36]

To study the temperature-dependent structure transitions of P3DDT, we first take a close look at the DSC thermogram shown in Fig. 1b. Two transitions are clearly seen in the heating run. The transition at higher temperatures (∼140–170 °C) is bimodal and due to the melting of an ordered phase and a less ordered phase,[17] and by comparing the first and second heating runs it is clear that most of the crystallinity present in the pristine P3DDT film is of the less-ordered phase. The endothermic peak centered at a lower temperature of ∼60 °C has been presumed to be side chain melting,[17,18] but conclusive evidence from structural analysis experiments is not yet available to the best of our knowledge.

In order to investigate the structure evolution associated with this transition, temperature-dependent FTIR spectroscopy was employed. Fig. 2a shows the C–H stretching and the $(CH_2)_n$ in-phase rocking regions of the FTIR spectrum of P3DDT at room temperature. In the 3000–2800 cm^{-1} region, the predominant

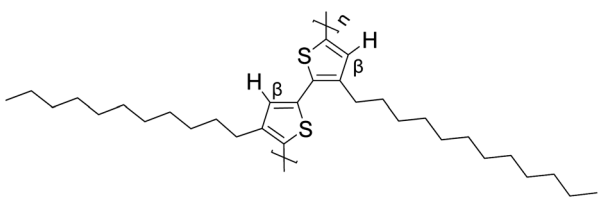

Scheme 1 Chemical structure of regioregular P3DDT.

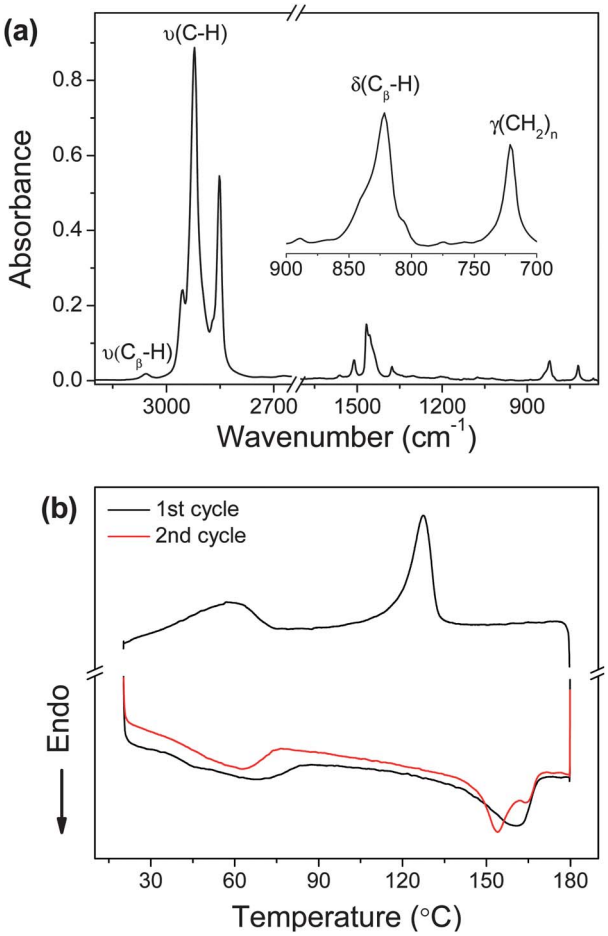

Fig. 1 (a) FTIR spectrum of P3DDT film at room temperature. The inset is an enlarged view of the 900–700 cm^{-1} region. (b) DSC thermogram of P3DDT film.

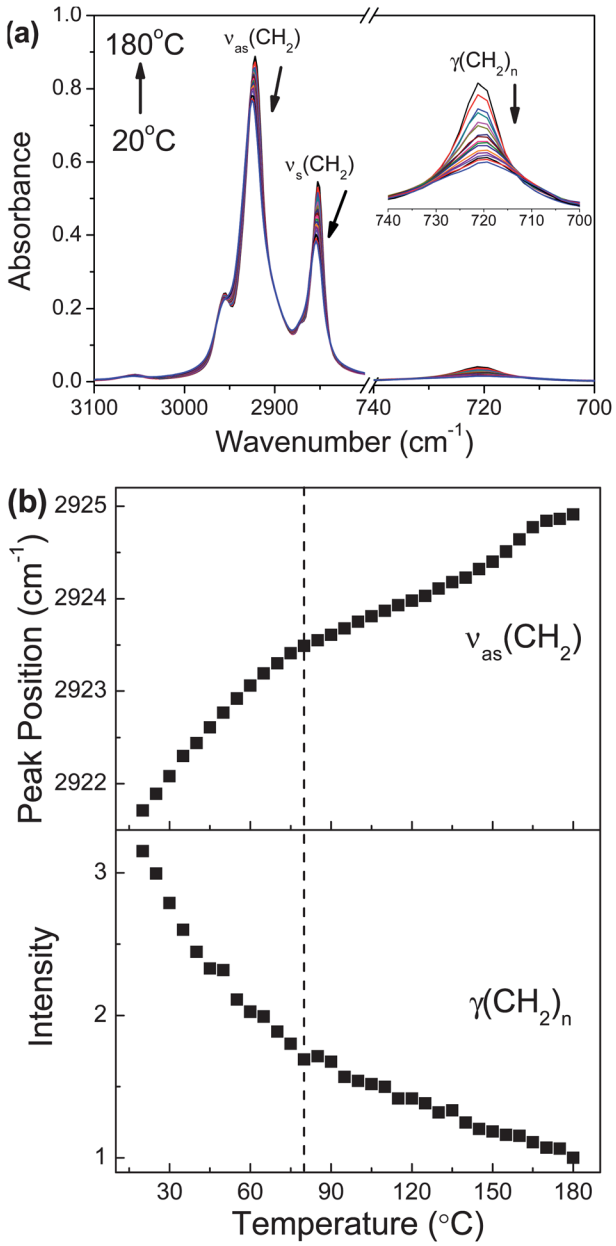

Fig. 2 (a) Temperature-dependent FTIR spectra of P3DDT film in the ranges of 3200–2800 cm^{-1} and 740–700 cm^{-1} for a heating run of 20–180 °C. The arrows mark the directions of change. (b) Peak position of the $\nu_{as}(CH_2)$ band and relative intensity of the $\gamma(CH_2)_n$ band for P3DDT as functions of temperature. The dash line marks 80 °C.

modes are the CH_2 asymmetric ($\nu_{as}(CH_2)$) and symmetric ($\nu_s(CH_2)$) stretchings located at ~2922 and ~2850 cm^{-1} respectively, characteristic of the alkyl side chains. The peak positions of these CH_2 stretching bands are known to be sensitive to the packing of *n*-alkane chains, and would shift to higher wavenumbers when the alkyl chains become more disordered.[37] Fig. 2b plots the peak position of the $\nu_{as}(CH_2)$ band as a function of temperature for the P3DDT film. It can be seen that the band located at ~2922 cm^{-1} at room temperature shifts upon heating to higher frequencies, with a clear turning point at ~80 °C. A similar trend was also observed for the $\nu_s(CH_2)$ band (not shown). Another band of interest is the $(CH_2)_n$ in-plane rocking ($\gamma(CH_2)_n$) band at ~720 cm^{-1}, which is also associated with the side chain, and the intensity of which decreased with temperature, with a distinct turning point also at ~80 °C. These spectral variations were completely reversed in the cooling process, with corresponding turning points observed at ~80 °C as well (ESI†). The presence of these turning points is convincing evidence that the transitions observed at this temperature range by DSC are the melting/crystallization of the P3DDT side chains. Furthermore, at room temperature the $\nu_{as}(CH_2)$ band is located at ~2922 cm^{-1}, close to but slightly higher than the value reported for all-*trans* chains in *n*-alkane crystals, 2920 cm^{-1},[38] indicating that the packing of the alkyl side chains is not as perfect and close as that in *n*-alkane crystals, whereas at 180 °C it is at ~2925 cm^{-1}, approaching but lower than the value of 2928 cm^{-1} for *n*-alkane liquids.[38] These results suggest that, unlike the traditional melting of *n*-alkane crystals, the side chain melting is a transition from a less perfect "crystal" to a "liquid" with some order. This is consistent with the fact that the alkyl side chains are fixed to a rigid main chain and thus can neither pack comfortably into perfect crystals nor move freely in the melt. Due to the same restriction effect, the size of the alkyl side chain domains are very

small with a wide distribution.[39] For these two reasons, the transition appears as a continuous change with a turning point rather than a discontinuous transformation.

Next we investigate the C_β-H out-of-plane bending ($\delta(C_\beta$-H)) band at ~870–800 cm^{-1}, which contains rich information about multiple structures of P3ATs.[28,33] Fig. 3 displays temperature-dependent FTIR spectra in the 900–790 cm^{-1} region for the heating process. Four bands are immediately identified at 890, 836, 820, and 806 cm^{-1}, which all vary with temperature. According to the literature, the small band at 890 cm^{-1} is assigned to methyl rocking of alkanes.[40,41] The dominant features in this region, the $\delta(C_\beta$-H) bands at 836 and 820 cm^{-1}, have been observed for P3ATs with shorter alkyl side chains and are associated with disordered and ordered forms of the main chain respectively.[11,28,32] DSC data (Fig. 1b) reveal different degrees of crystallinity in the first and second heating runs, yet the $\delta(C_\beta$-H) band for the film at 20 °C prior to each heating appears similar with three discernable components (inset, Fig. 3), although the peak maximum are slightly different, suggesting that the component at 820 cm^{-1} includes both ordered and less-ordered parts attributed to form I. This together with their intensity variations will be discussed further later. In addition to the three bands discussed, a small shoulder band is observed at ~806 cm^{-1}. This is a new spectral feature that has not been reported before for P3ATs. This band decreases upon heating and disappears at ~80 °C, and re-emerges at the same temperature upon cooling. Based on its temperature-dependency, this new band is preliminarily correlated to side-chain melting/crystallization. On the other hand, the intensity of this new band is comparable to that of the methyl rocking at 890 cm^{-1}, yet in this region crystallized alkanes exhibit only some bands belonging to splitting of methylene rocking modes, which are much weaker than the methyl rocking band.[40,41] Therefore this band cannot be ascribed to a vibrational mode of the alkyl side chains. The assignment of this band will be discussed in more detail later.

The temperature-dependent IR spectra for the 870–790 cm^{-1} region are analyzed by generalized 2D correlation spectroscopy.

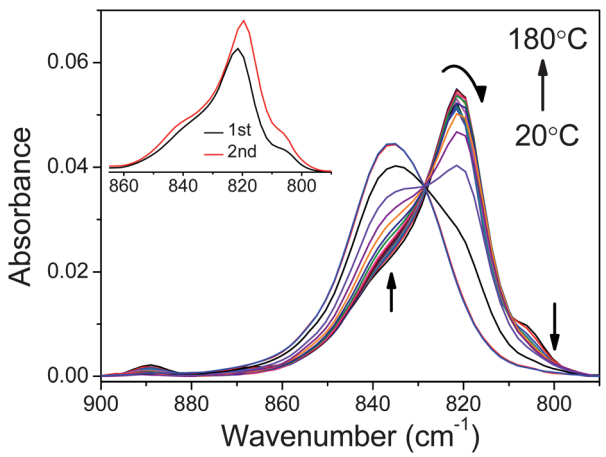

Fig. 3 Temperature-dependent FTIR spectra of P3DDT film in the 900–790 cm^{-1} range for a heating run of 20–180 °C. The arrows mark the directions of change. In the inset are spectra at 20 °C before the first and second heatings.

The technique, brought forward first by Noda and widely used since then, is capable of identifying overlapping bands and obtaining sequential order of events.[42–44] Presence of an autopeak, located on the diagonal, is indicative of intensity changes with the perturbation of the corresponding band, whereas the band that remains constant develops little or no autopeak. The off-diagonal peaks are referred as crosspeaks; a positive crosspeak indicates that the two bands it correlates are either increasing or decreasing together, and a negative one means that the two bands vary in opposite. Fig. 4 shows the synchronous contour plots of this region for the temperature variations of 20–70 and 80–150 °C, respectively. From positions of the autopeaks and crosspeaks in all these plots, it is obvious that in the 870–790 cm^{-1} region only three components are present, at 836, 820 and 806 cm^{-1}, respectively, same as that identified from Fig. 3, again implying that the ordered phase and the less-ordered phase observed by DSC cannot be distinguished by IR, and the band at 820 cm^{-1} represents both. In addition, the fact that correlation peaks for the 806 cm^{-1} band are observed only at 20–70 °C (Fig. 4a,c) and are totally absent at higher temperatures (Fig. 4b,d) is consistent with our assessment that this band is related to side-chain melting. For the first heating (Fig. 4a,b), in the temperature range 20–70 °C, the crosspeaks (836/806) and (820/806) are negative, and (836/820) is positive, indicating that while the 806 cm^{-1} band is decreasing, both 820 and 836 cm^{-1} bands are growing; at higher temperatures of 80–150 °C, the crosspeak (836/820) is negative, consistent with 820 cm^{-1} decreasing and 836 cm^{-1} increasing. The synchronous contour plot for the second heating in the temperature range of 80–150 °C is essentially the same as that for first heating, but in the temperature range 20–70 °C (Fig. 4c) they are rather different. The autopeak for 820 cm^{-1} is absent, and its crosspeaks are very weak, indicative of a near constant 820 cm^{-1} band during the temperature variation. Meanwhile, a negative crosspeak (836/806) means that while the band at 806 cm^{-1} is diminishing, 836 cm^{-1} is growing. The result that the band at 820 cm^{-1} increases at 20–70 °C along with side-chain melting during first heating is interesting and worth further investigation.

Fig. 5a plots the peak maximum of the broad $\delta(C_\beta$-H) band as a function of temperature. It can be seen that the peak maximum starts to shift to lower wavenumbers at ~60 °C in the first heating, but remains constant from 20 to 90 °C for first cooling and second heating. To better understand the origin of the components of this band, curve fitting of the spectra in the 870–790 cm^{-1} range is performed, and their variation with temperature studied. On the basis of 2D correlation analysis, the broad band is decomposed into three components, at 806, 820 and 836 cm^{-1}, respectively. Fig. 5b shows the curve-fitting result for the spectrum at 20 °C. The positions of the 836 and 806 cm^{-1} components barely vary, but the component at 820 cm^{-1} shifts with temperature (ESI†). The peak heights of these three components are plotted against temperature in Fig. 5c. From these curves, two critical temperatures can be identified at around 80 and 150 °C, corresponding to the meltings of the side chains and the main chains, respectively. In the first heating, the peak height of the 820 cm^{-1} component, associated with ordered main chain structures, barely changes at below 60 °C and then grows at 60–90 °C. This trend is consistent with that revealed by 2D analysis discussed above. The shift of the peak maximum to

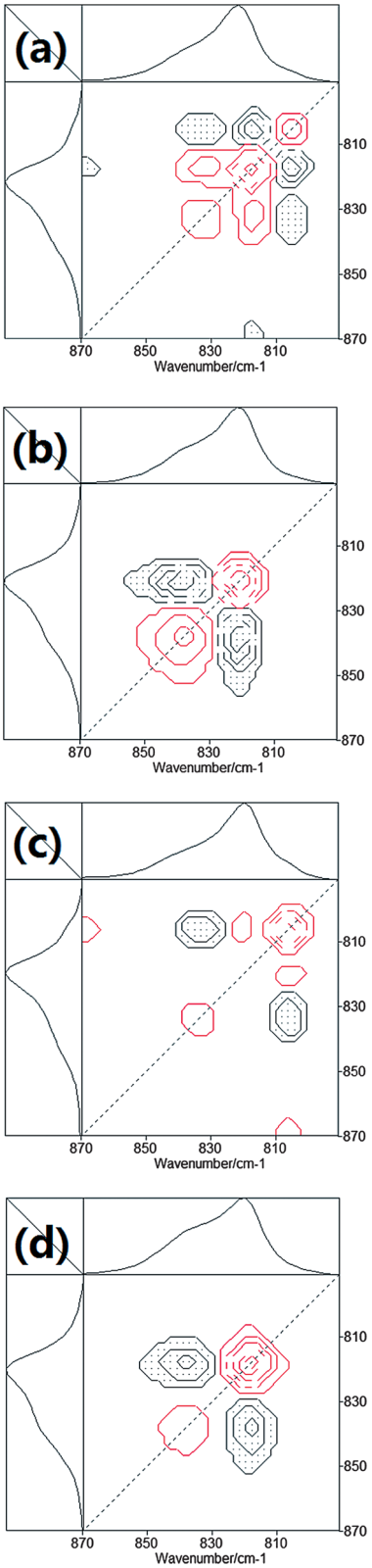

Fig. 4 Synchronous 2D correlation spectra of P3DDT films in the 870–790 cm^{-1} range for temperature variation of (a and c) 20–80 °C and (b and d) 80–150 °C during first heating (a and b) and second heating (c and d). Positive and negative correlation intensities are denoted by unshaded area (red) and shaded area (black) respectively.

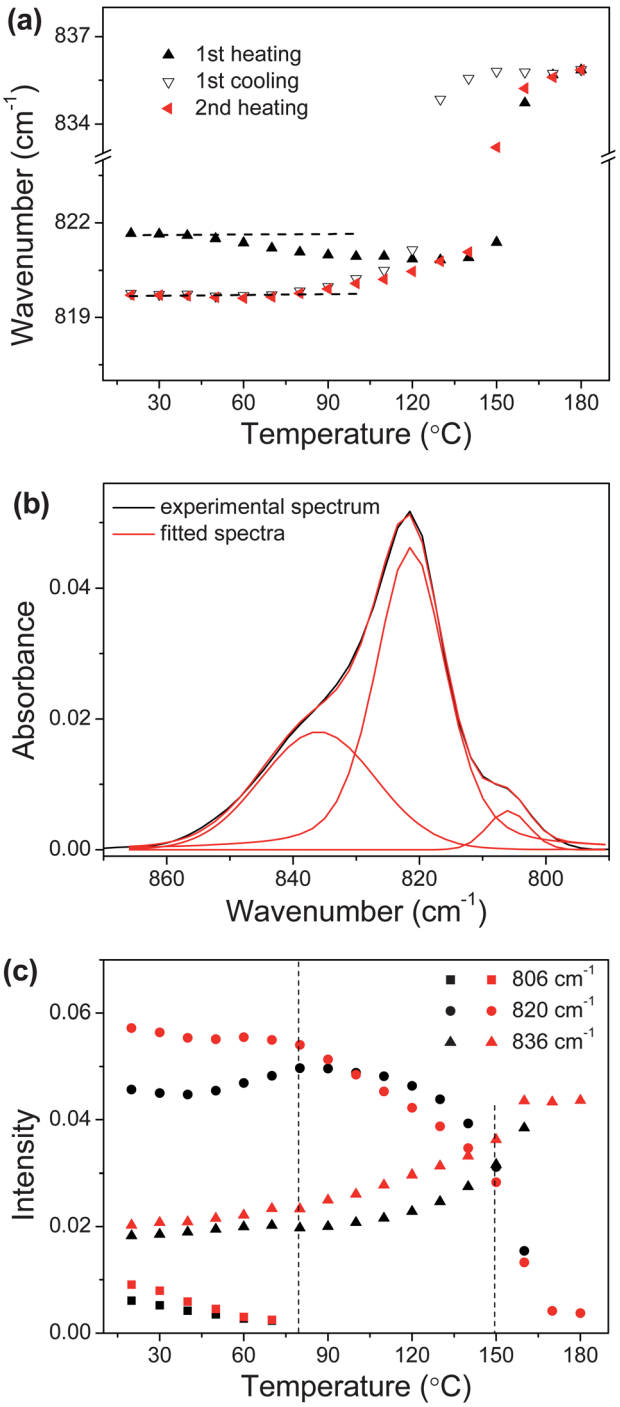

Fig. 5 (a) Variation of frequency at peak maximum of $\delta(C_\beta\text{-H})$ with temperature. (b) Curve fitting for the $\delta(C_\beta\text{-H})$ region. (c) Intensities of the three components of $\delta(C_\beta\text{-H})$ as functions of temperature for the first (black) and second (red) heatings. The dash lines are to guide the eye.

lower wavenumbers at above 60 °C together with the intensity increase of the 820 cm^{-1} component in the same temperature range suggests that upon melting of the side chains, rearrangement happens in the ordered phase. After the first cycle, the intensity of the 820 cm^{-1} component (at the beginning of the second heating) relative to that of 836 cm^{-1} has increased

significantly, indicating a higher crystallinity than that in the as-cast film. Then in the second heating, the 806 cm^{-1} band decreases gradually and completely disappears at ~80 °C, the temperature of side-chain melting, and in this temperature range the 836 cm^{-1} component increases, meanwhile the 820 cm^{-1} component barely changes or even decreases slightly. These results together indicate that the structure associated with the 806 cm^{-1} band transforms into an amorphous phase (836 cm^{-1}) directly, at temperatures much below the melting of the main chains in this structure, therefore the main chain must be disordered as well, yet its temperature-dependency correlates this band with side chain crystallinity as discussed in previous section. In the literature, alkyl nanodomains have been widely reported for comblike copolymers with long alkyl side chains regardless of the structure of the main chains,[39,45,46] including regioregular and regiorandom P3DDT.[19,20] Therefore based on all these results, it is reasonable to assign this band at 806 cm^{-1} to C_β-H out-of-plane bending of disordered thienyl chains with ordered alkyl side chains. It is likely that in this phase the side chains crystallize not in total but only the outer part to accommodate the frustration from the disordered main chains, as indicated by the position of the $\nu_{as}(CH_2)$ band discussed above.

Solvent evaporation rate in film fabrication and solvent vapor treatment on films prepared can significantly influence the microstructure of P3AT films.[25,28] Prolonged solvent evaporation in P3AT film preparation leads to doping[47] and formation of form II structure.[23] In this work, two films of P3DDT were prepared at different rates of solvent evaporation. The results discussed so far were obtained with films dried in ambience, denoted S1 hereafter; a different film, S2, was obtained by drying the solution in darkness in a sealed vessel *via* slow evaporation of the solvent over a period of several days. Fig. 6a compares the XRD patterns of these two P3DDT films. The pattern for S1 confirms that it is form I polymorph. In the XRD pattern of S2, in addition to the (100), (200), (300) peaks characteristic of form I of P3DDT, there is an inconspicuous peak at $2\theta = 4.4°$ next to the (100) peak of form I, which confirms the presence of form II in S2.[23,48] FTIR spectra of these two films are shown in Fig. 6b. In the 1300–1000 cm^{-1} region, two extra bands are observed at 1260 and 1090 cm^{-1} respectively for S2, which according to literature are assigned to doped segments of P3DDT caused by oxygen and moisture in the atmosphere,[35] apparently due to long drying time at ambience of S2. Of greater interest is the 870–690 cm^{-1} region, where a distinct peak emerges at 827 cm^{-1} that has not been reported in the literature. As seen in Fig. 7a, upon heating S2 from 20 to 90 °C, the intensity of this component is reduced and disappears at ~90 °C; at the same time, the intensity of 820 cm^{-1} increases. As the film is heated further and cooled down again, the band at 827 cm^{-1} does not reappear (Fig. 7b, c). It has been confirmed by XRD that form II transforms to form I on heating, and then disappears at higher temperature and does not re-emerge on cooling.[23,48] Based on this unique temperature-dependent behavior, we assign the band at 827 cm^{-1} to C_β-H out-of-plane bending of form II. So far XRD has been the only technique that can detect the presence of form II, and its characteristic diffraction, as seen in Fig. 6a, is very weak; in contrast, for the same specimen the 827 cm^{-1} band is the strongest in the 870–690 cm^{-1} region of the spectrum. Thus this vibrational band

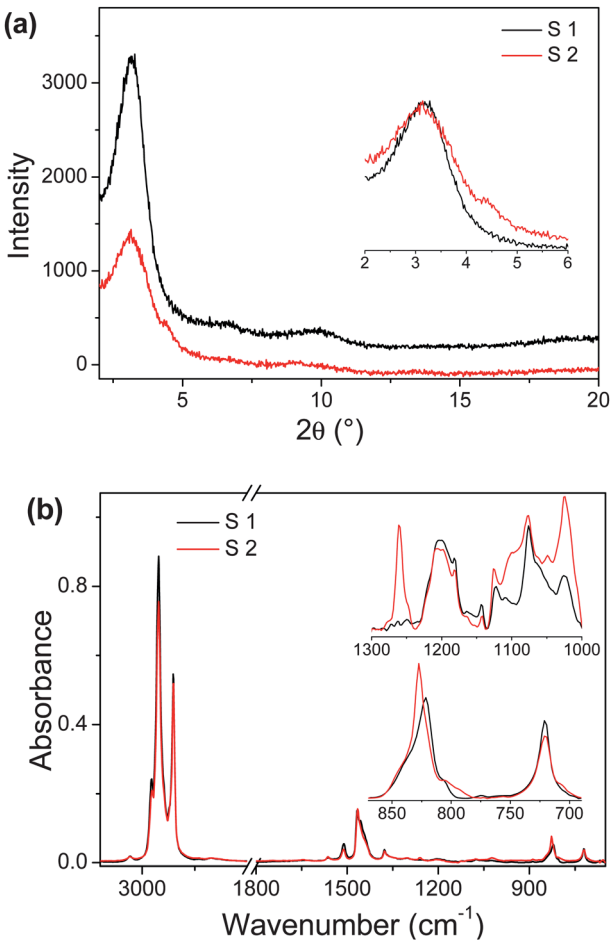

Fig. 6 (a) XRD patterns of P3DDT films S1 and S2 and (b) FTIR spectra of S1 and S2. The insets are the enlarged views.

at 827 cm^{-1} provides a new, convenient and sensitive way to identify and study form II in P3DDT films. In addition, another new band is observed at 800 cm^{-1} in the spectra of S2, which is absent in the spectrum of S1. The intensity of this band remains rather constant during heating and cooling, same as that of 1260 and 1090 cm^{-1} bands which are due to doped P3DDT segments.[35] We attribute this new band at 800 cm^{-1} to C_β-H out-of-plane bending of doped P3DDT segments.

Now the microstructure of P3DDT and its evolution with temperature can be discussed. At room temperature, three phases are present: the form I crystalline phase is characterized by the 820 cm^{-1} band; the disordered phase (836 cm^{-1}) where both the main chains and side chains are disordered, and an intermediate phase (806 cm^{-1}), in which the main chains are twisted and the side chains are aligned and ordered. A fourth phase, form II crystalline phase (827 cm^{-1}), may also be present depending on the preparation condition. Upon heating, the ordered side chains start to melt, and become completely disordered at ~80 °C; the ordered main chains also become more twisted gradually, and at ~150 °C transform into a disordered state. When the polymer is cooled from the melt, the process is reversed except the formation of form II. This is illustrated in Scheme 2.

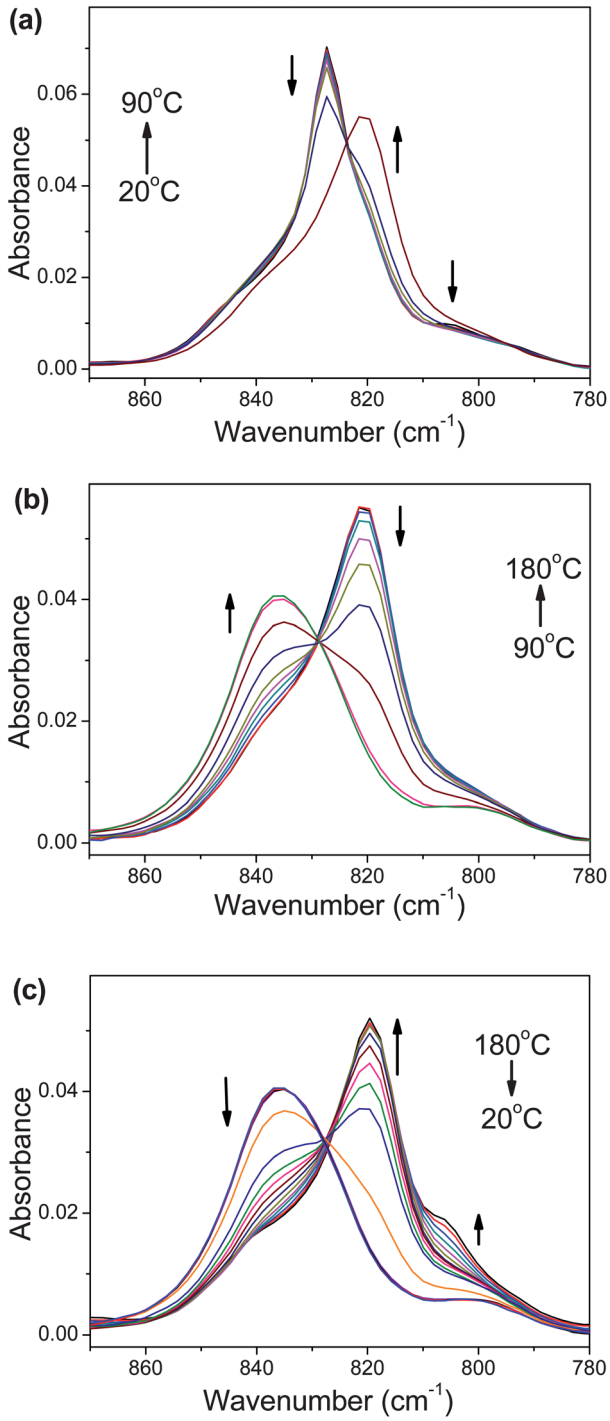

Fig. 7 Temperature-dependent FTIR spectra of S2 in the $\delta(C_\beta\text{-H})$ region for (a) 20–90 °C, (b) 90–180 °C, and (c) 180–20 °C.

Conclusions

In this work, microstructure and phase transitions of P3DDT have been investigated by temperature-dependent FTIR in conjugation with DSC and XRD, and vibrational bands characteristic of various structures of P3DDT have been established. Temperature-dependent FTIR analysis confirmed that the endothermic transition at ~80 °C is the melting of the side chains. New components of the C_β-H out-of-plane bending mode of the main chain located at 806, 827, and 800 cm^{-1} have been identified and assigned. The small band at 806 cm^{-1} is associated with the phase with crystalline side chains and disordered main chain, the peak at 827 cm^{-1} is due to the less-common form II crystal modification, and the 800 cm^{-1} component is ascribed to doped segments. With the aid of these new spectroscopic tools, the temperature-dependent phase structure of P3DDT is well described. The findings provide new insights into microstructures and phase transitions of P3DDT as well as other P3ATs, which may guide the processing of polythiophene materials for better performance in various applications.

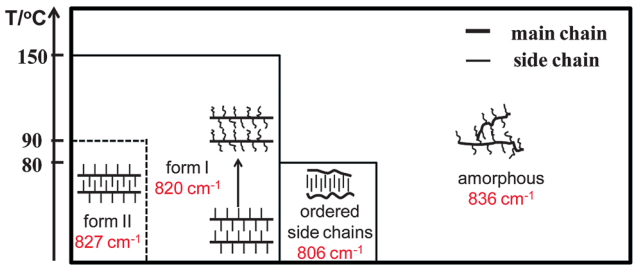

Scheme 2 Temperature-dependent structure of P3DDT films.

Acknowledgements

The financial support from the National Natural Science Foundation of China (20990233) is acknowledged. Z.S. thanks the NSFC Fund for Creative Research Groups (50921062) for support.

Notes and references

1 J. Roncali, *Chem. Rev.*, 1992, **92**, 711–738.
2 R. D. McCullough, *Adv. Mater.*, 1998, **10**, 93–116.
3 I. Osaka and R. D. McCullough, *Acc. Chem. Res.*, 2008, **41**, 1202–1214.
4 L. H. Nguyen, H. Hoppe, T. Erb, S. Gunes, G. Gobsch and N. S. Sariciftci, *Adv. Funct. Mater.*, 2007, **17**, 1071–1078.
5 W. D. Oosterbaan, J. C. Bolsee, A. Gadisa, V. Vrindts, S. Bertho, J. D'Haen, T. J. Cleij, L. Lutsen, C. R. McNeill, L. Thomsen, J. V. Manca and D. Vanderzande, *Adv. Funct. Mater.*, 2010, **20**, 792–802.
6 X. N. Yang, J. Loos, S. C. Veenstra, W. J. H. Verhees, M. M. Wienk, J. M. Kroon, M. A. J. Michels and R. A. J. Janssen, *Nano Lett.*, 2005, **5**, 579–583.
7 H. Sirringhaus, P. J. Brown, R. H. Friend, M. M. Nielsen, K. Bechgaard, B. M. W. Langeveld-Voss, A. J. H. Spiering, R. A. J. Janssen, E. W. Meijer, P. Herwig and D. M. de Leeuw, *Nature*, 1999, **401**, 685–688.
8 R. J. Kline, M. D. McGehee, E. N. Kadnikova, J. S. Liu, J. M. J. Frechet and M. F. Toney, *Macromolecules*, 2005, **38**, 3312–3319.
9 X. Yang, G. Lu, L. Li and E. Zhou, *Small*, 2007, **3**, 611–615.
10 O. Inganas, W. R. Salaneck, J. E. Osterholm and J. Laakso, *Synth. Met.*, 1988, **22**, 395–406.
11 G. Zerbi, B. Chierichetti and O. Inganas, *J. Chem. Phys.*, 1991, **94**, 4646–4658.
12 C. Yang, F. P. Orfino and S. Holdcroft, *Macromolecules*, 1996, **29**, 6510–6517.
13 S. Malik and A. K. Nandi, *J. Polym. Sci., Part B: Polym. Phys.*, 2002, **40**, 2073–2085.
14 V. Causin, C. Marega, A. Marigo, L. Valentini and J. M. Kenny, *Macromolecules*, 2005, **38**, 409–415.

15 A. Zen, M. Saphiannikova, D. Neher, J. Grenzer, S. Grigorian, U. Pietsch, U. Asawapirom, S. Janietz, U. Scherf, I. Lieberwirth and G. Wegner, *Macromolecules*, 2006, **39**, 2162–2171.
16 Z. Y. Wu, A. Petzold, T. Henze, T. Thurn-Albrecht, R. H. Lohwasser, M. Sommer and M. Thelakkat, *Macromolecules*, 2010, **43**, 4646–4653.
17 K. C. Park and K. Levon, *Macromolecules*, 1997, **30**, 3175–3183.
18 S. L. Liu and T. S. Chung, *Polymer*, 2000, **41**, 2781–2793.
19 S. Pankaj and M. Beiner, *J. Phys. Chem. B*, 2010, **114**, 15459–15465.
20 S. Pankaj, E. Hempel and M. Beiner, *Macromolecules*, 2009, **42**, 716–724.
21 Y. Guo, Y. Jin and Z. Su, *Polym. Chem.*, 2012, DOI: 10.1039/c2py00582d.
22 M. Brinkmann, *J. Polym. Sci., Part B: Polym. Phys.*, 2011, **49**, 1218–1233.
23 T. J. Prosa, M. J. Winokur and R. D. McCullough, *Macromolecules*, 1996, **29**, 3654–3656.
24 S. V. Meille, V. Romita, T. Caronna, A. J. Lovinger, M. Catellani and L. Belobrzeckaja, *Macromolecules*, 1997, **30**, 7898–7905.
25 G. H. Lu, L. G. Li and X. N. Yang, *Adv. Mater.*, 2007, **19**, 3594–3598.
26 J. Liu, Y. Sun, X. Gao, R. Xing, L. Zheng, S. Wu, Y. Geng and Y. Han, *Langmuir*, 2011, **27**, 4212–4219.
27 P. Arosio, M. Moreno, A. Famulari, G. Raos, M. Catellani and S. V. Meille, *Chem. Mater.*, 2009, **21**, 78–87.
28 Y. Yuan, J. M. Zhang and J. Q. Sun, *Macromolecules*, 2011, **44**, 6128–6135.
29 Y. Yuan, J. M. Zhang, J. Q. Sun, J. Hu, T. P. Zhang and Y. X. Duan, *Macromolecules*, 2011, **44**, 9341, DOI: 10.1021/ma2017106.
30 G. Zerbi, B. Chierichetti and O. Inganas, *J. Chem. Phys.*, 1991, **94**, 4637–4645.
31 K. Tashiro, K. Ono, Y. Minagawa, M. Kobayashi, T. Kawai and K. Yoshino, *J. Polym. Sci., Part B: Polym. Phys.*, 1991, **29**, 1223–1233.
32 K. Yazawa, Y. Inoue, T. Yamamoto and N. Asakawa, *Phys. Rev. B*, 2006, **74**, 094204.
33 K. Yazawa, Y. Inoue, T. Yamamoto and N. Asakawa, *J. Phys. Chem. B*, 2008, **112**, 11580–11585.
34 K. Yazawa, Y. Inoue, T. Shimizu, M. Tansho and N. Asakawa, *J. Phys. Chem. B*, 2010, **114**, 1241–1248.
35 G. Louarn, M. Trznadel, J. P. Buisson, J. Laska, A. Pron, M. Lapkowski and S. Lefrant, *J. Phys. Chem.*, 1996, **100**, 12532–12539.
36 H. Hagemann, H. L. Strauss and R. G. Snyder, *Macromolecules*, 1987, **20**, 2810–2819.
37 H. Tachibana, N. Hosaka and Y. Tokura, *Macromolecules*, 2001, **34**, 1823–1827.
38 R. G. Snyder, H. L. Strauss and C. A. Elliger, *J. Phys. Chem.*, 1982, **86**, 5145–5150.
39 M. Beiner and H. Huth, *Nat. Mater.*, 2003, **2**, 595–599.
40 R. G. Snyder, *J. Mol. Spectrosc.*, 1960, **4**, 411–434.
41 R. G. Snyder, *J. Mol. Spectrosc.*, 1961, **7**, 116–144.
42 Q. Jia, N. N. Wang and Z. W. Yu, *Appl. Spectrosc.*, 2009, **63**, 344–353.
43 I. Noda, *J. Mol. Struct.*, 2010, **974**, 3–24.
44 I. Noda, *Appl. Spectrosc.*, 1993, **47**, 1329–1336.
45 H. F. Shi, Y. Zhao, X. Q. Zhang, S. C. Jiang, D. J. Wang, C. C. Han and D. F. Xu, *Macromolecules*, 2004, **37**, 9933–9940.
46 H. F. Shi, Y. Zhao, X. Q. Zhang, Y. Zhou, Y. Z. Xu, S. R. Zhou, D. J. Wang, C. C. Han and D. F. Xu, *Polymer*, 2004, **45**, 6299–6307.
47 H.-H. Liao, C.-M. Yang, C.-C. Liu, S.-F. Horng, H.-F. Meng and J.-T. Shy, *J. Appl. Phys.*, 2008, **103**, 104506.
48 T. J. Prosa, J. Moulton, A. J. Heeger and M. J. Winokur, *Macromolecules*, 1999, **32**, 4000–4009.

